A Novel Dual-Band Transmission Line With Equal-Phase Responses

Mohammadreza Rezvani Pakdeh, Ali Tajik, and Mohammad Fakharzadeh, *Senior Member, IEEE*

***Abstract*— This article presents a novel dual-band transmission line (TL), consisting of a multibranch stub, which can provide equal unwrapped phases at two different frequencies. The frequency ratio can be close to one without any significant degradation in the device performance. Besides, the bandwidth of the proposed line can be manipulated at both frequencies by adjusting the design parameters. The behavior of the structure over the frequency bands is investigated theoretically, and the design procedure and relations are derived. The simulation and measurement results of a quarter-wavelength open-ended stub and a branch-line coupler (BLC) are presented and compared to verify the performance of the proposed dual-band TL. It is shown that the first structure has a simulated and measured insertion phase of 90° at 2 and 3 GHz. The BLC is designed for 4G and 5G applications with two center frequencies of 3.52 and 4.78 GHz, resulting in a frequency ratio of 1.36. The measured insertion loss values at these frequencies are 3.8 and 3.2 dB, the coupled port loss values are 3.5 and 3.1 dB, and the output phase differences are 91.7° and 92.8°, respectively.**

***Index Terms*— Branch-line coupler (BLC), dual-band, equal phase, 4G/5G, multibranch stub, transmission line (TL).**

I. Introduction

THE dual-band structures are used to combine two or more frequency applications in one device, for example, LTE and new 5G frequency bands [1]. Usually, the dual-band structures have a smaller size and are cost-effective compared with two single-band devices, while they preserve a similar performance at both desired frequency bands.

Considering that many microwave components are based on transmission lines (TLs), for example, couplers, one of the common design methods for a dual-band structure is to design a dual-band TL. In this way, composite right-/left-handed (CRLH) TLs are widely used to convert the conventional microwave components into dual-band devices [2]–[4]. Another design method is to use the lumped *LC* elements to design a compact dual-band structure [5]. However, the desired frequency response may not be achieved exactly. Finally, adding open-/short-ended stubs to the TL is another way to achieve the dual-band performance [6]–[9]. In all these cases, only the 90° TL is investigated, and other phases are ignored.

Manuscript received August 11, 2020; revised October 19, 2020; accepted October 28, 2020. Date of publication January 14, 2021; date of current version February 4, 2021. *(Corresponding author: Mohammad Fakharzadeh.)*

The authors are with the Electrical Engineering Department, Sharif University of Technology, Tehran 11365-11155, Iran (e-mail: mhreza.rezvani@gmail.com; ali.tajik92@yahoo.com; fakharzadeh@sharif.edu).

Color versions of one or more figures in this article are available at https://doi.org/10.1109/TMTT.2020.3040732.

Digital Object Identifier 10.1109/TMTT.2020.3040732

In addition, in [8], the ability to control the bandwidth at the desired frequency bands by adjusting the insertion phase variation is introduced. The open-ended stubs can be combined with stepped-impedance sections to form a dual-band TL [10], while Gai *et al.* [11] use dual TLs. The main idea of [6]–[11] is to manipulate the ABCD matrix of the achieved TL to be similar to a quarter-wavelength TL at two distinct frequencies.

There are heuristic dual-band design methods that are developed for a specific component, such as a branch-line coupler (BLC). Mostly, the structure is modified in different ways. For example, the equivalent lumped circuit models of the circular patches are used in [12], and the whole structure is examined with the even–odd mode technique to achieve a dual-band BLC. With the same technique, cross-coupled branches, which connect the corners of BLC to each other, are utilized in [13]. The even–odd mode analysis is widely used to design a dual-band BLC, such as the design in [14]–[16]. In [14], the regular branches of the BLC are replaced by the coupled lines, and in [15], the conventional BLC is loaded with coupled line stubs to achieve dual-band operation. In addition, it has been shown that a dual-band BLC could be designed by adding extra stubs to the center of the vertical branches [16] or to the corners of the conventional BLC [17]. Extending the feed ports of the single-band BLC is another approach to change the structure in order to exhibit the dual-band performance [18]. A systematic design technique utilizing T- and Π-networks is presented in [19] for designing a dual-band BLC and crossover. Finally, in [20], a multiband BLC, which is designed by adding open-ended stubs to a conventional BLC, is reported.

In this article, a novel dual-band TL with a multibranch stub is presented, which is illustrated in Fig. 1. The novelties of this work are as follows. The proposed structure can be designed for any arbitrary equal unwrapped phase at two arbitrary frequencies, while previous works have focused on the TLs with wrapped ±90° phases [2]–[11]. Another feature of the proposed structure is preserving the desired performance particularly at two close frequencies contrary to the previous work, particularly CRLH-based structures [21].

The organization of this article is given as follows. In Section II, the origin of the idea and the behavior of the proposed dual-band TL are introduced with the possibility of achieving an equal phase at two desired frequencies. Section III discusses the design procedure of the proposed TL, using straightforward and linear relations. This section is continued by analyzing the impedance behavior of the TL, the capability of phase variation control, and the flexibility of

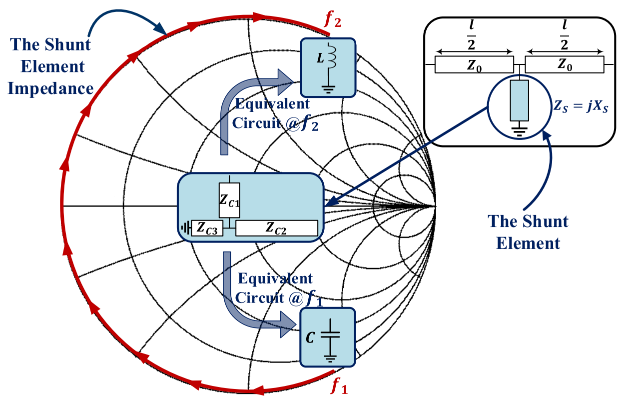

Fig. 1. Frequency behavior of the proposed multibranch stub used in the equal-phase TL.

the design parameters. Section IV presents the simulation and measurement results of the two sample structures based on the proposed TL, followed by the conclusion.

II. Theory

This section discusses the effect of loading a TL section with a shunt element and derives the S-parameters of the proposed structure. Fig. 1 depicts a TL section with the length of l, the propagation constant of β, and the characteristic impedance of Z_0 loaded with a shunt element with the impedance of Z_S, which is placed at the center of the TL section. The ABCD matrix of the whole structure for $Z_S = jX_S$ is

$$\begin{bmatrix} A_T & B_T \\ C_T & D_T \end{bmatrix} = \begin{bmatrix} \cos\left(\frac{\beta l}{2}\right) & jZ_0\sin\left(\frac{\beta l}{2}\right) \\ \frac{j\sin\left(\frac{\beta l}{2}\right)}{Z_0} & \cos\left(\frac{\beta l}{2}\right) \end{bmatrix} \times \begin{bmatrix} 1 & 0 \\ \frac{1}{jX_S} & 1 \end{bmatrix} \begin{bmatrix} \cos\left(\frac{\beta l}{2}\right) & jZ_0\sin\left(\frac{\beta l}{2}\right) \\ \frac{j\sin\left(\frac{\beta l}{2}\right)}{Z_0} & \cos\left(\frac{\beta l}{2}\right) \end{bmatrix}. \tag{1}$$

The elements of the matrix are calculated to be

$$\begin{cases} A_T = D_T = \cos(\beta l) + \dfrac{Z_0}{2X_S}\sin(\beta l) \\ B_T = \dfrac{{Z_0}^2}{j2X_S}(\cos(\beta l) - 1) + jZ_0\sin(\beta l) \\ C_T = \dfrac{j}{Z_0}\sin(\beta l) + \dfrac{\cos(\beta l) + 1}{j2X_S}. \end{cases} \tag{2}$$

Let the reference impedance be the characteristics impedance of the TL section (Z_0). The S-parameters of the structure are

$$S_{11} = \frac{j\frac{Z_0}{2X_S}}{\cos(\beta l) + j\sin(\beta l) - \frac{Z_0}{2X_S}(j\cos(\beta l) - \sin(\beta l))} \tag{3}$$

$$S_{21} = \frac{1}{\cos(\beta l) + j\sin(\beta l) - \frac{Z_0}{2X_S}(j\cos(\beta l) - \sin(\beta l))}. \tag{4}$$

From (3), the magnitude of the reflection coefficient can be simplified as

$$|S_{11}| = \sqrt{\left(\frac{\left(\frac{Z_0}{2X_S}\right)^2}{1 + \left(\frac{Z_0}{2X_S}\right)^2}\right)}. \tag{5}$$

Also, the insertion phase could be obtained from (4) as

$$\angle S_{21} = -\left(\beta l - \tan^{-1}\left(\frac{Z_0}{2X_S}\right)\right). \tag{6}$$

If $|(Z_0/2X_S)| \ll 1$, then from (5)

$$|S_{11}| \simeq \left|\frac{Z_0}{2X_S}\right|. \tag{7}$$

Also, using (6) and considering

$$\tan^{-1}\left(\frac{Z_0}{2X_S}\right) \simeq \frac{Z_0}{2X_S} \tag{8}$$

results in

$$\angle S_{21} \simeq -\left(\beta l - \frac{Z_0}{2X_S}\right). \tag{9}$$

When $|(Z_0/2X_S)| < 0.33$, $|S_{11}|$ is less than -10 dB, and the error of the approximation in (8) is less than 3.6 % error.

From (9), it is seen that the phase response of the whole line consists of two distinct parts:

1) the phase of the TL section (βl);
2) an added phase caused by the shunt element ($-(Z_0/2X_S)$).

Inherently, in a nondispersive medium, β has a linear relation with the frequency. Thus, when the frequency increases, the phase of the TL section increases proportionally. Thus, for two different frequencies denoted by f_1 and f_2, where $f_1 < f_2$, the absolute phase of the TL section at f_2 is higher than its phase at f_1. On the contrary, the added phase caused by the shunt element could be either negative or positive, considering the sign of X_S, which depends on the nature of the shunt element. Thus, it is possible to achieve an equal total phase at f_1 and f_2 with a TL section loaded with the shunt element. It is desirable that the shunt element behaves as a capacitive load at f_1 to increase the phase lag of the structure, while it behaves as an inductive load at f_2 to mitigate the phase lag, as shown in Fig. 1. Thereby, it is possible that such a structure has exactly equal unwrapped phases at both frequencies by controlling the impedance of the shunt element.

III. Design Procedure

In this section, the idea of utilizing the shunt element to compensate for the phase lag of the TL section over the desired frequency band is explained. By rewriting (9) at two arbitrary frequencies, it is seen that the phase response of the structure can be manipulated by exploiting a proper shunt element to achieve an equal phase at both frequencies.

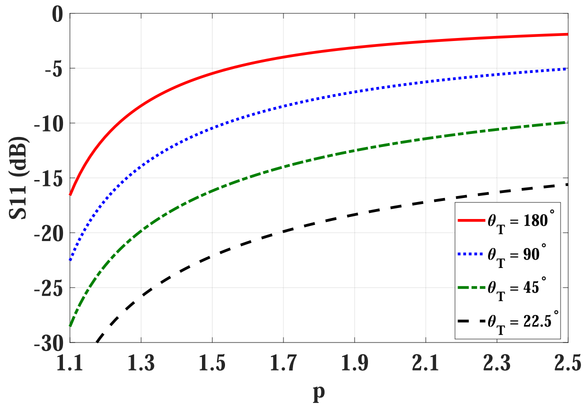

Fig. 2. Reflection coefficient of the proposed dual-band TL versus frequency ratio (p) for different values of an electrical length (θ_T).

A. Equal-Phase Transmission Line Design

Let θ_T denote the desired equal phase of the structure at both frequencies. Then, (9) is rewritten at f_1 and f_2 as

$$\begin{cases} \theta_R \; + x = \theta_T, & @\, f_1 \\ p\theta_R - x = \theta_T, & @\, f_2 \end{cases} \tag{10}$$

where θ_R is the phase of the TL section at f_1, p is the frequency ratio ($p = (f_2/f_1)$), and x is the added phase at f_1 and the subtracted phase at f_2, which is caused by the shunt element. Thus, according to (9), x is

$$x = -\frac{Z_0}{2X_S(f_1))} = \frac{Z_0}{2X_S(f_2))}. \tag{11}$$

As it is noted in (11), the added phase at f_1 and the subtracted phase at f_2 are decided to be equal so that $|S_{11}|$ has the same value at both f_1 and f_2, based on (7) and (9).Then, the equation set of (10) can be solved to find θ_R and x, which yields

$$\theta_R = \frac{2}{p+1}\theta_T \tag{12}$$

$$x = \frac{p-1}{p+1}\theta_T. \tag{13}$$

Considering (5) and (13), $|S_{11}|$ values at f_1 and f_2 are

$$|S_{11}|(f_1) = |S_{11}|(f_2) = \sqrt{\frac{(p-1)^2\theta_T^2}{(p+1)^2 + (p-1)^2\theta_T^2}}. \tag{14}$$

Also, the impedance of the shunt element can be calculated from (11) as

$$Z_S(f_1) = -j\frac{Z_0}{2x} \tag{15}$$

$$Z_S(f_2) = j\frac{Z_0}{2x}. \tag{16}$$

Using (14), the reflection coefficient of the proposed dual-band TL is plotted versus p for four values of θ_T in Fig. 2. It is seen that the impedance matching improves when p or θ_T decreases. Therefore, the proposed structure is particularly suitable for dual-band applications, where the two frequency bands are close.

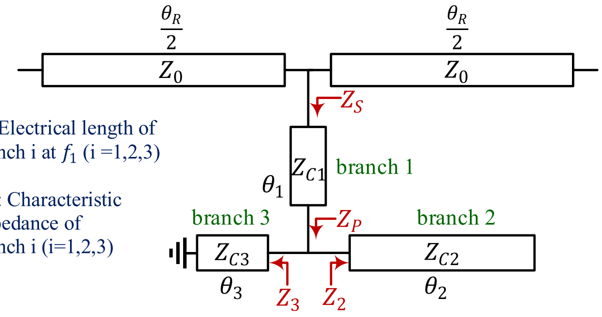

Fig. 3. Proposed dual-band TL with the multibranch stub. All electrical lengths are defined at f_1.

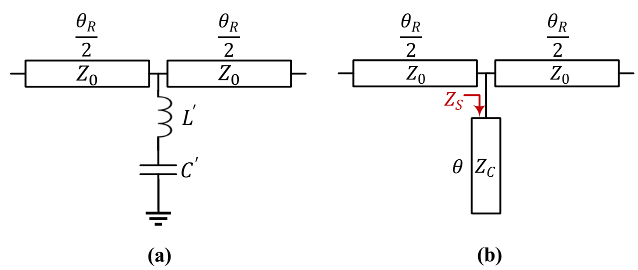

Fig. 4. Two possible solutions for the shunt element. (a) Series LC resonator. (b) Single open-ended stub. All electrical lengths are defined at f_1.

B. Proposed Circuit for the Shunt Element

The proposed circuit for the shunt element is a multibranch stub, as shown in Fig. 3, which satisfies the mentioned properties of the shunt element, but it is not the unique solution. Before investigating this structure, it is helpful to examine two intuitive solutions.

The first possible solution is a series LC resonator, as shown in Fig. 4(a), which is capacitive at the lower and inductive at the higher frequencies than the resonance frequency. Inevitably, the lumped elements may degrade the performance by adding parasitic elements and self-resonance especially at higher frequencies and increase the assembly costs. Besides, it may not be possible to find off-the-shelf components with the desired values.

The next solution is to use open-ended stub, which could be implemented in two configurations, i.e., Π-shape [22] and T-shape [7], with an electrical length smaller than 90° at f_1 (capacitive impedance) and larger than 90° at f_2 (inductive impedance). The T-shape structure is shown in Fig. 4(b), where Z_C is the characteristic impedance and θ is the electrical length of the stub at f_1. Considering the open stub impedance [$Z_S = -jZ_C \cot((f\theta/f_1)))$] and equating it to the proper impedances in (15) and (16), after some mathematical simplifications, Z_C and θ are obtained as

$$\theta = \frac{\pi}{p+1} \tag{17}$$

$$Z_C = \frac{Z_0(p+1)\tan\left(\frac{\pi}{p+1}\right)}{2(p-1)\theta_T}. \tag{18}$$

From (18), it is seen that, for p values, which are close to 1, Z_C becomes extremely large and, thus, impossible to fabricate the corresponding line on PCB. For example, if a 20-mil RO4003C substrate is used as the PCB substrate, for $f_1 = 2$ GHz, $f_2 = 2.5$ GHz, and $\theta_T = 90°$, then $Z_C = 451\ \Omega$, which corresponds to a microstrip line with less than 1 µm width. Thus, in this case, the use of a single open-ended stub is not practical for any p value. However, this idea can be extended to a multibranch stub, as shown in Fig. 3, where the design parameters are defined inside the figure. In this case, there are more degrees of freedom available to design a realizable structure. Indeed, Z_{C1}, Z_{C2}, and Z_{C3} can be chosen in such a way that the corresponding branches can be realized using a regular PCB process even though the value of p becomes close to one.

Let $Z_P(f) = Z_2(f)||Z_3(f)$, where

$$Z_2(f) = -jZ_{C2}\cot\left(\frac{f}{f_1}\theta_2\right) \tag{19}$$

$$Z_3(f) = jZ_{C3}\tan\left(\frac{f}{f_1}\theta_3\right). \tag{20}$$

To implement the inductive shunt element at f_2, the electrical length of the branch 2 is presumed to be$(\pi/2)$ at f_2, or

$$\theta_2 = \frac{\pi}{2p} \tag{21}$$

which causes Z_P to be zero independent of branch 3. Therefore, branch 1 becomes a short-ended stub. Its electrical length is calculated from (16)

$$j\frac{Z_0}{2x} = jZ_{C1}\tan(p\theta_1) \rightarrow \theta_1 = \frac{1}{p}\tan^{-1}\left(\frac{Z_0}{2xZ_{C1}}\right). \tag{22}$$

To obtain the electrical length of branch 3, first, $Z_S(f)$ is written as

$$Z_S(f) = Z_{C1}\frac{Z_P(f) + jZ_{C1}\tan\left(\frac{f}{f1}\theta_1\right)}{Z_{C1} + jZ_P(f)\tan\left(\frac{f}{f1}\theta_1\right)}. \tag{23}$$

By equating (23) at f_1 to (15) and after doing mathematical simplifications, $Z_3(f_1)$ is derived as

$$Z_3(f_1) = \frac{jZ_{C1}}{\frac{Z_{C1}}{Z_{C2}\cot(\theta_2)} - \frac{(2xZ_{C1}-Z_0\tan(\theta_1))}{(Z_0+2xZ_{C1}\tan(\theta_1))}} \tag{24}$$

and, consequently, θ_3 is obtained as

$$\theta_3 = \tan^{-1}\left(\frac{Z_3(f_1)}{jZ_{C3}}\right). \tag{25}$$

As an example, a dual-band 90° TL is designed utilizing the proposed multibranch stub assuming that $f_1 = 2$ GHz and $f_2 = 2.5$ GHz. Following the design procedure, from (12) and (13), θ_R and x are obtained to be 80° and 10°, respectively. Considering Section II, the calculated value of x in this example is smaller than 0.33 rad, which satisfies the constraint of (8). Moreover, for implementing the shunt element with multibranch stub, Z_{C1}, Z_{C2}, and Z_{C3} are chosen arbitrarily to be 80 Ω, and then, by using (22) and (25), θ_1, θ_2, and θ_3 are calculated to be 48.65°, 72° and 16.25°, respectively. The calculated reflection coefficient and insertion phase of this line are shown in Fig. 5, which indicates that a 90° phase is achieved at both frequencies, while retaining a proper value for $|S_{11}|$, which is −15.29 dB.

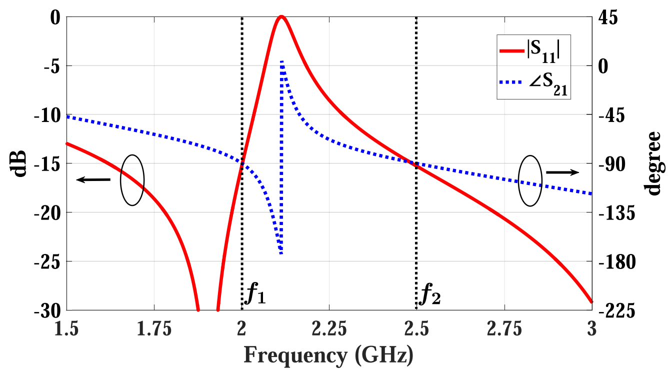

Fig. 5. Calculated reflection coefficient and insertion phase of the proposed dual-band TL for $Z_{C1} = Z_{C2} = Z_{C3} = 80\ \Omega$, $\theta_T = 90°$, $f_1 = 2$ GHz, and $f_2 = 2.5$ GHz.

C. Multibranch Stub Impedance Behavior

To elaborate on the behavior of the multibranch stub, its impedance is derived versus frequency. From (23), $Z_S(f)$ can be simplified using trigonometric identities, as

$$Z_S(f) = -jZ_{C1}\cot\left(\frac{f\theta_1}{f_1} + \theta_{\text{eff}}(f)\right) \tag{26}$$

where

$$\theta_{\text{eff}}(f) = \tan^{-1}\left(\frac{Z_{C1}}{Z_{C2}}\tan\left(\frac{f\theta_2}{f_1}\right) - \frac{Z_{C1}}{Z_{C3}}\cot\left(\frac{f\theta_3}{f_1}\right)\right). \tag{27}$$

From (26), the total impedance of the multibranch stub is similar to the impedance of a single open-ended stub with total electrical length of $(f/f_1)\theta_1 + \theta_{\text{eff}}(f)$ and with the characteristics impedance of Z_{C1}. Moreover, $\theta_{\text{eff}}(f)$ is defined as the effective electrical length of branch 2 and branch 3, which are parallel.

D. Degrees of Freedom in the Design Procedure

Based on Section III-B, Z_{C1}, Z_{C2}, and Z_{C3} form the degrees of freedom in the proposed design that can be selected arbitrarily. Also, θ_2 can be changed as another degree of freedom. These parameters could be used to manipulate the performance or size of the structure.

1) Phase Slope Manipulation: Insertion phase variation is important in dual-band applications because it influences the phase stability over the desired frequency bands, and consequently, it determines the useful bandwidth of the dual-band TLs, in addition to the reflection coefficient criterion. According to (26) and (27), the behavior of Z_S is mainly dependent on Z_{C1}. Therefore, the variation of Z_{C1} affects the insertion phase variation of the proposed dual-band TL. To examine this effect qualitatively, the example in Fig. 5 is redesigned with different values of Z_{C1}, and the insertion phases are calculated and plotted in Fig. 6. It is seen that the insertion phase slope increases at f_1 and decreases at f_2 as Z_{C1} increases. To investigate the stability of the insertion phase of a dual-band 90° TL at f_1 and f_2, it is helpful to define a figure of merit ($\Delta f_{90°}$) for both frequencies as

$$\Delta f_{90°} = f_{100°} - f_{80°} \tag{28}$$

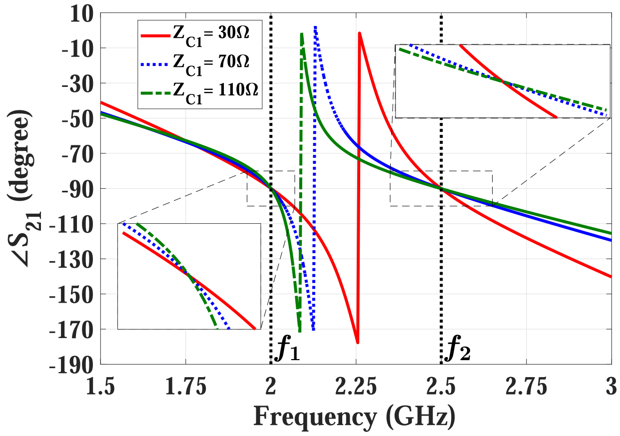

Fig. 6. Calculated insertion phase of the proposed dual-band TL versus Z_{C1} for $\theta_T = 90°$ and $Z_{C2} = Z_{C3} = 80\ \Omega$.

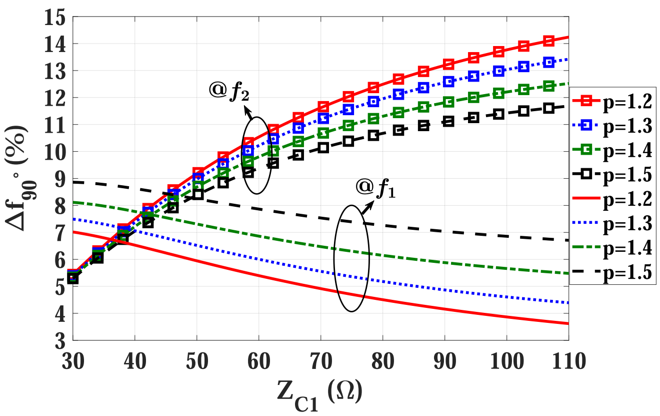

Fig. 7. Calculated $\Delta f_{90°}$ for the proposed dual-band TL versus Z_{C1} for different values of p, assuming that $\theta_T = 90°$ and $Z_{C2} = Z_{C3} = 80\ \Omega$.

where $f_{100°}$ and $f_{80°}$ are the frequencies around the center frequency, where the insertion phase is 100° and 80°, respectively. Fig. 7 shows the values of $\Delta f_{90°}$ versus Z_{C1} for a dual-band 90° TL section, assuming Z_{C2} and Z_{C3} are 80 Ω. Fig. 7 suggests that $\Delta f_{90°}$ decreases at f_1 and increases at f_2 as Z_{C1} increases, which is inversely proportional to the insertion phase slope. $\Delta f_{90°}$ is an applicable criterion to control the bandwidth of the dual-band BLCs.

2) Flexibility in the Length of Branches: According to Section III-B, in the multibranch stub design, the electrical length of branch 2 is 90° at f_2 to make Z_P zero, which leads to a straightforward solution for calculation of θ_1 and θ_3. However, θ_2 can be reduced, as another degree of freedom, to manipulate the length of the branches. For other values of θ_2, the corresponding values of θ_1 and θ_3 can be obtained by equating Z_S in (26) to the impedances in (15) and (16), or

$$\begin{cases} -jZ_{C1}\cot(\theta_1 + \theta_{\text{eff}}(f_1)) = -j\dfrac{Z_0}{2x}, & @\, f_1 \\ -jZ_{C1}\cot(p\theta_1 + \theta_{\text{eff}}(f_2)) = j\dfrac{Z_0}{2x}, & @\, f_2. \end{cases} \tag{29}$$

Following the example in Fig. 5, the equation set of (29) is solved for different values of θ_2 assuming that $Z_{C1} = 100\ \Omega$ and $Z_{C2} = Z_{C3} = 30\ \Omega$. Then, the corresponding values of θ_1 and θ_3 are calculated in Table I, which shows that the length of the branches is flexible parameter in the proposed design.

TABLE I

PARAMETERS OF THE MULTIBRANCH STUB WITH DIFFERENT VALUES OF θ_2 ($\theta_T = 90°$, $f_1 = 2$ GHz, AND $f_2 = 2.5$ GHz)

Parameter	Design 1	Design 2	Design 3	Design 4
$p\theta_2$	90°	80°	70°	60°
$p\theta_1$	55.08°	59.32°	65.87°	74.68°
$p\theta_3$	22.17°	31.61°	40.44°	48.34°

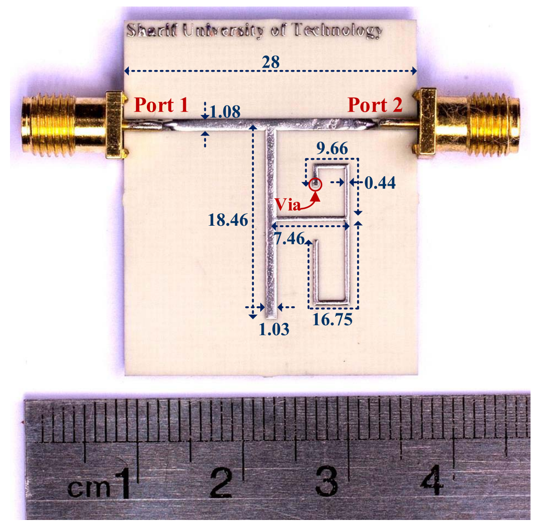

Fig. 8. Fabricated TL loaded with the proposed dual-band quarter-wavelength TL. All dimensions are in mm.

TABLE II

DUAL-BAND BLC DESIGN PARAMETERS

Parameter	θ_R	x	θ_1	θ_2	θ_3
$Z_0 = 50\ \Omega$	77.27°	12.73°	41.05°	67.69°	21.52°
$Z_0 = 35.355\ \Omega$	77.27°	12.73°	33.72°	67.69°	24.11°

IV. EXPERIMENTAL RESULTS

To evaluate the proposed dual-band structure with the multibranch stub design, two structures are designed and simulated by ANSYS HFSS. These circuits are fabricated using RO4003C substrate (20-mil thickness and $\epsilon_r = 3.55$) and measured with a network analyzer.

A. Dual-Band Quarter-Wavelength TL

The first structure is a dual-band 90° TL designed for $f_1 = 2$ GHz and $f_2 = 3$ GHz with the frequency ratio of $p = 1.5$. Using (12) and (13), θ_R and x are obtained to be 72° and 18°, respectively. x is smaller than 0.33 rad, which satisfies (8). The value of Z_{C1}, Z_{C2}, and Z_{C3} could be chosen arbitrarily, but, considering the practical limits, the value of 80 Ω is selected for all three impedances. Thus, θ_1, θ_2, and θ_3 are calculated to be 29.90°, 60°, and 34.42°, respectively.

TABLE III
COMPARING THE PERFORMANCE OF THE PROPOSED BLC WITH OTHER WORKS

	f_1, f_2 (GHz)	f_2/f_1	$\|S_{11}\|$ (dB)	$\|S_{21}\|$ (dB)	$\|S_{31}\|$ (dB)	$\angle S_{21} - \angle S_{31}$ (°)	Bandwidth (%) ($\|S_{11}\| < -10$ dB)
[3]	1, 2	2	-20.38, -24.19	-4.29, -3.8	-4.33, -4.54	*-90.6, 88	*12.5, 13.7
[6]	2.4, 5.74	2.39	*-28.5, -37	-3.57, -4.06	-3.62, -4.23	*89.5, -91.6	*19.1, 9.2
[11]	0.87, 1.79	2.06	-26, -21.6	-3.3, -3.09	-3.67, -3.9	89.3, 91.4	*14.1, 20.9
[14]	2, 4	2	-20, -20	-3.7, -5	-3.7, -3.8	86.5, 84.3	*38.2, 15.8
[15]	0.76, 1.42	1.87	-15, -15	-3.35, -3.74	-4, -4.1	-89.1, 89.6	*20.2, 12.2
[18]	1, 2	2	-36.7, -25.3	-3.3, -3.1	-3.1, -3.7	90, 89	*25.9, 12.8
This work	3.52, 4.78	1.36	-18.6, -23.38	-3.78, -3.24	-3.51, -3.11	91.7, 92.8	7.9, 20.2

*Estimated from the graphs in the paper

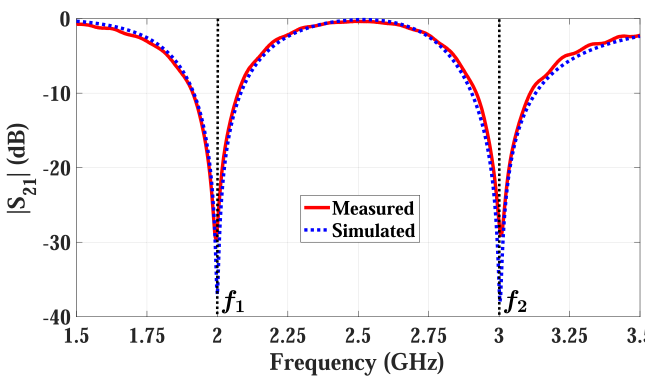

Fig. 9. Simulated and measured $|S_{21}|$ of the TL loaded with the proposed dual-band 90° TL as an open-ended stub.

To demonstrate that the total phase of the dual-band TL is 90° at both frequencies, it is connected as an open-ended stub, to a conventional microstrip line, which is shown in Fig. 8. Therefore, it is anticipated that some nulls appear in $|S_{21}|$ of the whole structure at the frequencies, where the dual-band stub becomes quarter-wavelength.

Fig. 9 compares the simulation and measurement results of this structure, where two nulls in $|S_{21}|$ curve are observed at 2 and 3 GHz. It implies that the 90° phase is achieved by the dual-band TL with the multibranch stub at the designed frequencies.

B. Dual-Band Branch Line Coupler

The second structure shown in Fig. 10 is a dual-band BLC, designed for 3.4–3.6- and 4.4–5-GHz bands, which corresponds to 4G band 42 [23] and 5G-n79 band [24], respectively. To design this BLC, the conventional 90° lines of the single-band BLC are replaced with the dual-band 90° TLs with the operational frequencies of $f_1 = 3.5$ GHz and $f_2 = 4.7$ GHz ($p \simeq 1.34$), which are considered to be the center frequencies of the desired bands. As mentioned in Section III-D, the value of Z_{C1} controls the bandwidth of the TL. Thus, the value of Z_{C1} is chosen 80 Ω, the same as Z_{C2} and Z_{C3}, to cover the required bandwidth referring to Fig. 7. A procedure similar to the first structure design

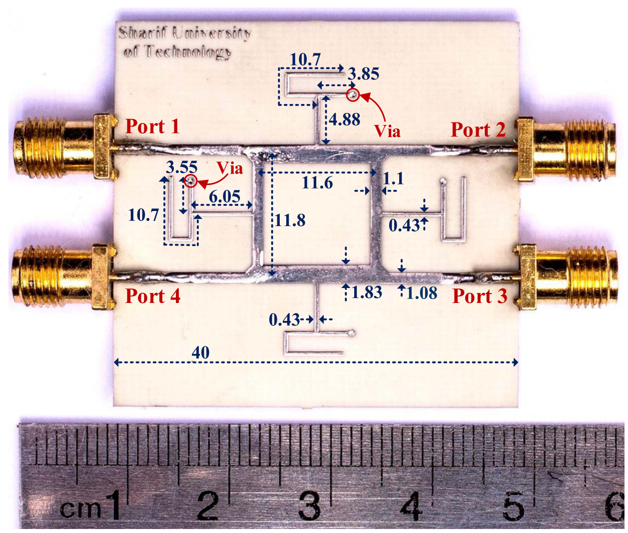

Fig. 10. Fabricated structure of the dual-band BLC using the proposed dual-band TL. All dimensions are in mm.

is followed for designing the TLs of the BLC, which yields the calculated values in Table II for 50- and 35.35-Ω TLs. According to Table II, x is smaller than 0.33 rad, which satisfies the approximation in (8).

The simulated and measured S-parameters of this BLC are depicted in Fig. 11(a) and (b), respectively. Fig. 11 implies that the desired performance is achieved at both frequencies considering the fact that the frequency ratio is close to 1. Table III compares this work with a similar work, which indicates that this work has the lowest frequency ratio, while preserving proper bandwidth at both frequencies. As a paramount criterion, the phase difference of the direct and coupled ports is near to 90° at both frequencies, whereas, in some of the other work [3], [6], [15], it is not 90°. This is an important issue in the phased array or switched array systems, such as the Butler matrix [25]. A reasonable return loss is obtained at both frequencies (better than 18 dB) in conjunction with the proper values for the insertion loss (better than 3.8 dB) with a low amplitude imbalance between the direct and coupled ports (less than 0.2 dB).

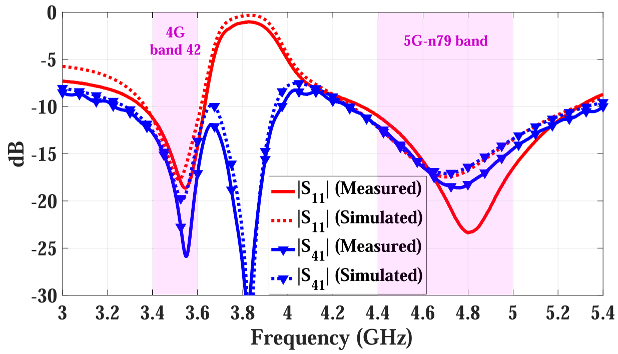

(a)

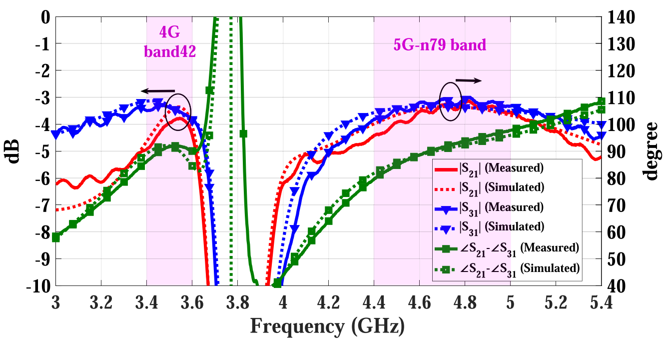

(b)

Fig. 11. Simulated and measured S-parameters of the dual-band BLC. (a) $|S_{11}|$ and $|S_{21}|$. (b) $|S_{41}|$, $|S_{31}|$, and $\angle S_{21} - \angle S_{11}$.

V. Conclusion

In this article, the effect of a shunt element on the phase response of a TL section, with the goal of achieving an equal insertion phase, is studied, and as a solution, the multibranch stub is proposed. The benefits of the proposed structure are studied, which can be summarized as the capability of achieving an equal phase response at two arbitrary frequencies, controlling the phase variation of the structure and designing dual-band circuits for two close frequencies. Moreover, a dual-band quarter-wavelength TL and a BLC were designed, fabricated, and measured successfully, to verify the performance of the proposed dual-band TL.

References

[1] G. Lv, W. Chen, X. Chen, F. M. Ghannouchi, and Z. Feng, "A compact Ka/Q dual-band GaAs MMIC Doherty power amplifier with simplified offset lines for 5G applications," *IEEE Trans. Microw. Theory Techn.*, vol. 67, no. 7, pp. 3110–3121, Jul. 2019.

[2] I.-H. Lin, M. DeVincentis, C. Caloz, and T. Itoh, "Arbitrary dual-band components using composite right/left-handed transmission lines," *IEEE Trans. Microw. Theory Techn.*, vol. 52, no. 4, pp. 1142–1149, Apr. 2004.

[3] P.-L. Chi and T. Itoh, "Miniaturized dual-band directional couplers using composite right/left-handed transmission structures and their applications in beam pattern diversity systems," *IEEE Trans. Microw. Theory Techn.*, vol. 57, no. 5, pp. 1207–1215, May 2009.

[4] O. Garcia-Perez, A. Garcia-Lamperez, V. Gonzalez-Posadas, M. Salazar-Palma, and D. Segovia-Vargas, "Dual-band recursive active filters with composite right/left-handed transmission lines," *IEEE Trans. Microw. Theory Techn.*, vol. 57, no. 5, pp. 1180–1187, May 2009.

[5] W.-T. Fang, E.-W. Chang, and Y.-S. Lin, "Bridged-T coil for miniature dual-band branch-line coupler and power divider designs," *IEEE Trans. Microw. Theory Techn.*, vol. 66, no. 2, pp. 889–901, Feb. 2018.

[6] K.-S. Chin, K.-M. Lin, Y.-H. Wei, T.-H. Tseng, and Y.-J. Yang, "Compact dual-band branch-line and rat-race couplers with stepped-impedance-stub lines," *IEEE Trans. Microw. Theory Techn.*, vol. 58, no. 5, pp. 1213–1221, May 2010.

[7] H. Zhang and K. J. Chen, "A stub tapped branch-line coupler for dual-band operations," *IEEE Microw. Wireless Compon. Lett.*, vol. 17, no. 2, pp. 106–108, Feb. 2007.

[8] K.-K.-M. Cheng and S. Yeung, "A novel dual-band 3-dB branch-line coupler design with controllable bandwidths," *IEEE Trans. Microw. Theory Techn.*, vol. 60, no. 10, pp. 3055–3061, Oct. 2012.

[9] A. M. Zaidi, B. K. Kanaujia, M. T. Beg, J. Kishor, and K. Rambabu, "A novel dual-band branch line coupler for dual-band butler matrix," *IEEE Trans. Circuits Syst. II, Exp. Briefs*, vol. 66, no. 12, pp. 1987–1991, Dec. 2019.

[10] C.-L. Hsu, J.-T. Kuo, and C.-W. Chang, "Miniaturized dual-band hybrid couplers with arbitrary power division ratios," *IEEE Trans. Microw. Theory Techn.*, vol. 57, no. 1, pp. 149–156, Jan. 2009.

[11] C. Gai, Y.-C. Jiao, and Y.-L. Zhao, "Compact dual-band branch-line coupler with dual transmission lines," *IEEE Microw. Wireless Compon. Lett.*, vol. 26, no. 5, pp. 325–327, May 2016.

[12] S. Y. Zheng, Y. Wu, Y. Li, Y. Liu, and Y. Long, "Dual-band hybrid coupler with arbitrary power division ratios over the two bands," *IEEE Trans. Compon., Packag., Manuf. Technol.*, vol. 4, no. 8, pp. 1347–1358, Aug. 2014.

[13] M.-J. Park and B. Lee, "Dual-band, cross coupled branch line coupler," *IEEE Microw. Wireless Compon. Lett.*, vol. 15, no. 10, pp. 655–657, Oct. 2005.

[14] L. K. Yeung, "A compact dual-band 90○ coupler with coupled-line sections," *IEEE Trans. Microw. Theory Techn.*, vol. 59, no. 9, pp. 2227–2232, Sep. 2011.

[15] W. Feng, Y. Zhao, W. Che, H. Chen, and W. Yang, "Dual-/tri-band branch line couplers with high power division isolation using coupled lines," *IEEE Trans. Circuits Syst. II, Exp. Briefs*, vol. 65, no. 4, pp. 461–465, Apr. 2018.

[16] W. Feng, X. Duan, Y. Shi, X. Y. Zhou, and W. Che, "Dual-band branch-line couplers with short/open-ended stubs," *IEEE Trans. Circuits Syst. II, Exp. Briefs*, vol. 67, no. 11, pp. 2497–2501, Nov. 2020.

[17] P.-L. Chi and K.-L. Ho, "Design of dual-band coupler with arbitrary power division ratios and phase differences," *IEEE Trans. Microw. Theory Techn.*, vol. 62, no. 12, pp. 2965–2974, Dec. 2014.

[18] H. Kim, B. Lee, and M.-J. Park, "Dual-band branch-line coupler with port extensions," *IEEE Trans. Microw. Theory Techn.*, vol. 58, no. 3, pp. 651–655, Mar. 2010.

[19] M. A. Maktoomi, M. S. Hashmi, and F. M. Ghannouchi, "Systematic design technique for dual-band branch-line coupler using T- and pi-networks and their application in novel wideband-ratio crossover," *IEEE Trans. Compon., Packag., Manuf. Technol.*, vol. 6, no. 5, pp. 784–795, May 2016.

[20] C.-W. Tang and M.-G. Chen, "Design of multipassband microstrip branch-line couplers with open stubs," *IEEE Trans. Microw. Theory Techn.*, vol. 57, no. 1, pp. 196–204, Jan. 2009.

[21] C. Caloz and T. Itoh, *Electromagnetic Metamaterials: Transmission Line Theory Microwave Applications*. Hoboken, NJ, USA: Wiley, 2005.

[22] K.-K. M. Cheng and F.-L. Wong, "A novel approach to the design and implementation of dual-band compact planar 90° branch-line coupler," *IEEE Trans. Microw. Theory Techn.*, vol. 52, no. 11, pp. 2458–2463, Nov. 2004.

[23] (Jun. 2020). *LTE; Evolved Universal Terrestrial Radio Access (E-UTRA); User Equipment (UE) Radio Transmission and Reception V16.6.0*. [Online]. Available: https://portal.3gpp.org/desktopmodules/Specifications/SpecificationDeta% ils.aspx?specificationId=2411

[24] (Jul. 2020). *5G; NR; User Equipment (UE) Radio Transmission and Reception; Part 1: Range 1 Standalone V16.4.0*. [Online]. Available: https://portal.3gpp.org/desktopmodules/Specifications/Specification Deta% ils.aspx?specificationId=3283

[25] A. Tajik, A. S. Alavijeh, and M. Fakharzadeh, "Asymmetrical 4×4 butler matrix and its application for single layer 8 × 8 butler matrix," *IEEE Trans. Antennas Propag.*, vol. 67, no. 8, pp. 5372–5379, Aug. 2019.

Mohammadreza Rezvani Pakdeh received the B.Sc. and M.Sc. degrees in electrical engineering from the Sharif University of Technology, Tehran, Iran, in 2016 and 2019, respectively.

From 2017 to 2019, he worked on highly sensitive measurement systems at the Microwave and Millimeter Wave Lab, Sharif University of Technology. He is currently a member of the Mm-Wave Imaging Research Group, Sharif University of Technology, where he is involved in designing and implementing mm-wave imaging systems. His research interests include the design and implementation of RF/mm-wave circuits and systems.

Ali Tajik received the B.S. degree in electrical engineering from the University of Tehran, Tehran, Iran, in 2015, and the M.S. degree in communication, fields, and waves engineering from the Sharif University of Technology, Tehran, in 2018.

From 2013 to 2015, he worked on wireless power transfer using waveguide resonators at the Microwave Group, University of Tehran. His research interests include the design and implementation of active and passive RF, microwave and millimeter-wave components, and switched beam and frequency beam scanning array antennas.

Mohammad Fakharzadeh (Senior Member, IEEE) received the M.Sc. degree in electrical engineering from the Sharif University of Technology, Tehran, Iran, in 2002, and the Ph.D. degree (Hons.) in electrical and computer engineering (ECE) from the University of Waterloo, Waterloo, ON, Canada, in 2008.

He was the Manager of the Antenna and Packaging Group, Peraso Technologies, Toronto, ON, Canada, developing the integrated millimeter-wave solutions for portable electronic devices and small-cell backhaul. He is currently an Associate Professor with the Electrical Engineering Department, Sharif University of Technology, where he is also the Director of the Sharif University Incubator. He has over 18 years of experience in the design and implementation of the phased-array antenna and mm-wave systems, particularly novel antenna and packaging solutions. He has authored over 80 IEEE articles. He holds ten U.S. patents.